



Detection of RO₂ radicals and other products from cyclohexene ozonolysis with NH₄⁺ and acetate chemical ionization mass spectrometry

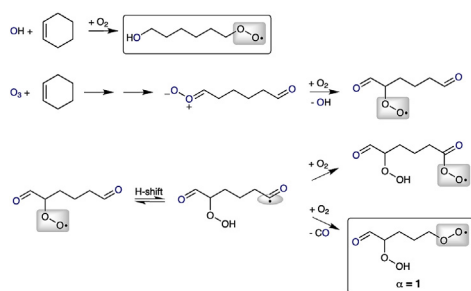
Armin Hansel^{a,b,*}, Wiebke Scholz^a, Bernhard Mentler^a, Lukas Fischer^a, Torsten Berndt^c

^a Institute for Ion Physics and Applied Physics, University of Innsbruck, Technikerstrasse 25, 6020, Innsbruck, Austria

^b Department of Physics, University of Helsinki, P.O. Box 64, Helsinki, 00014, Finland

^c Leibniz Institute for Tropospheric Research, TROPOS, 04318, Leipzig, Germany

GRAPHICAL ABSTRACT



ARTICLE INFO

Keywords:
RO₂ radicals
Cyclohexene
Ozonolysis
HOMs
CIMS
Carbon closure

ABSTRACT

The performance of the novel ammonium chemical ionization time of flight mass spectrometer (NH₄⁺-CI3-TOF) utilizing NH₄⁺ adduct ion chemistry to measure first generation oxidized product molecules (OMs) as well as highly oxidized organic molecules (HOMs) was investigated for the first time. The gas-phase ozonolysis of cyclohexene served as a first test system. Experiments have been carried out in the TROPOS free-jet flow system at close to atmospheric conditions. Product ion signals were simultaneously observed by the NH₄⁺-CI3-TOF and the acetate chemical ionization atmospheric pressure interface time of flight mass spectrometer (acetate-CI-API-TOF). Both instruments are in remarkable good agreement within a factor of two for HOMs. For OMs not containing an OOH group the acetate technique can considerably underestimate OM concentrations by 2–3 orders of magnitude. First steps of cyclohexene ozonolysis generate ten different main products, detected with the ammonium-CI3-TOF, comprising 93% of observed OMs. The remaining 7% are distributed over several minor products that can be attributed to HOMs, predominately to highly oxidized RO₂ radicals. Summing up, observed ammonium-CI3-TOF products yield 5.6×10^9 molecules cm⁻³ in excellent agreement with the amount of reacted cyclohexene of 4.5×10^9 molecules cm⁻³ for reactant concentrations of [O₃] = 2.25×10^{12} molecules cm⁻³ and [cyclohexene] = 2.0×10^{12} molecules cm⁻³ and a reaction time of 7.9 s. NH₄⁺ adduct ion chemistry is a promising CIMS technology for achieving carbon-closure due to the unique opportunity for complete detection of the whole product distribution including also peroxy radicals, and consequently, for a much better understanding of oxidation processes.

Abbreviations: NH₄⁺-CI3-TOF, NH₄⁺-Chemical Ionization 3 - Time of Flight; acetate-CI-API-TOF, Acetate-chemical ionization; atmospheric pressure interface, Time of Flight; OMs, Oxidized Product Molecules; HOMs, Highly Oxidized Organic Compounds; ELVOCs, Extremely Low Volatility Organic Compounds; SOA, Secondary Organic Aerosol; PTR-MS, Proton Transfer Reaction Mass Spectrometer

* Corresponding author. Institute for Ion Physics and Applied Physics, University of Innsbruck, Technikerstrasse 25, 6020, Innsbruck, Austria.

E-mail address: Armin.Hansel@uibk.ac.at (A. Hansel).

<https://doi.org/10.1016/j.atmosenv.2018.04.023>

Received 17 November 2017; Received in revised form 12 April 2018; Accepted 14 April 2018

Available online 17 April 2018

1352-2310/ © 2018 The Authors. Published by Elsevier Ltd. This is an open access article under the CC BY license (<http://creativecommons.org/licenses/by/4.0/>).

1. Introduction

Understanding the degradation mechanisms of hydrocarbons with highest biogenic emission rates, such as isoprene and terpenes (Guenther et al., 2012), is important to predict their contribution to the atmospheric oxidation budget and the importance of their oxidation products for particle nucleation and secondary organic aerosol (SOA) formation (Riipinen et al., 2012). Because of the important role that SOA plays in air quality and global climate, the formation of SOA components has been a major area of research in recent years. Despite these efforts we do not have a complete molecular level understanding how SOA is formed from precursor gases. In particular the chemistry and formation of extremely low volatility organic compounds (ELVOCs) currently represents one gap in our knowledge. Ehn et al. (2014) observed ELVOCs from gas-phase oxidation of α -pinene in a smog chamber, as well as from atmospheric measurements in a boreal forest (Ehn et al., 2012). ELVOCs are believed to contain hydroperoxy and carbonyl groups, and their vapor pressure is expected to be very low (Donahue et al., 2012). ELVOC formation can be explained by autooxidation of highly oxidized peroxy radicals (RO₂) (Ehn et al., 2014; Jokinen et al., 2014; Berndt et al., 2016). Ozonolysis experiments of the most abundant monoterpenes, α -pinene and limonene showed that highly oxidized RO₂ radicals with up to 12 O atoms and the corresponding closed shell products are formed by a step by step O₂ insertion initiated by intramolecular H-shifts of RO₂ radicals on a time scale of seconds (Jokinen et al., 2014; Crounse et al., 2013).

Two recent studies focused on the formation of these closed shell products starting from the ozonolysis of cycloalkenes (Rissanen et al., 2014; Mentel et al., 2015). Especially cyclohexene serves as model substance with an endocyclic double bond, which represents the reactive structural element of the most important monoterpenes α -pinene and limonene. The first steps of cyclohexene ozonolysis are given in Scheme 1 demonstrating the generation of two types of RO₂ radicals, i.e. O₂-C₆H_{9-x}(OOH)_xO₂ with x = 0, 1, ... and O-C₅H_{9- α} (OOH) _{α} O₂ with α = 1, 2, ...

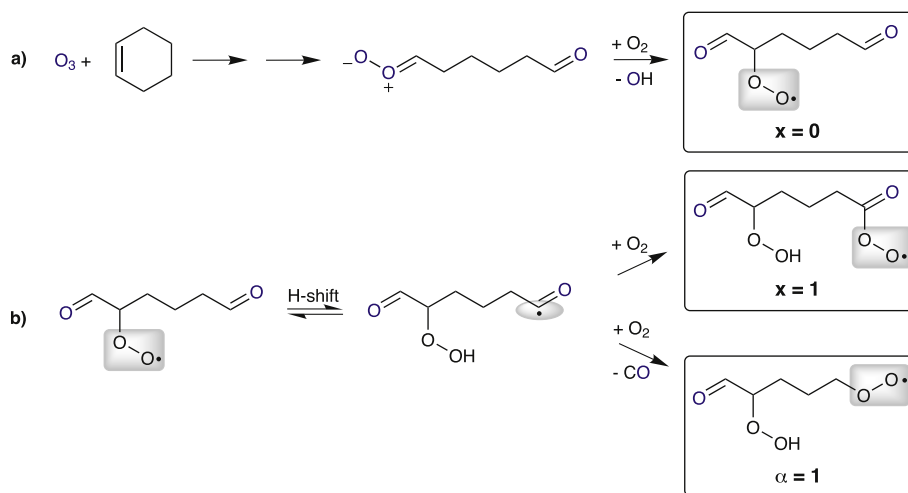
Berndt et al. (2015) studied very recently the formation of highly oxidized RO₂ radicals from C₅-C₈ cycloalkenes and their reactions with NO, NO₂, SO₂ and other RO₂ radicals. Up to now, highly oxidized RO₂ radicals and subsequent closed-shell products bearing at least five O atoms in the molecule could be detected in most cases by nitrate-CI-API-TOF mass spectrometry. Additional experiments using acetate as the reagent ion confirmed the existence of these highly oxidized RO₂ radicals and closed-shell products but failed to detect less-oxidized

products due to insufficient sensitivity (Berndt et al., 2015). While acetate ionization allows the detection of a broader range of products compared to the commonly used nitrate ionization, both techniques are unable to provide information on the whole product distribution. Very recently new methods for measurement of peroxy radicals (RO₂) focusing on less oxidized RO₂ were presented. Onel et al. (2017) developed a method for methyl peroxy (CH₃O₂) radical measurement using the conversion of CH₃O₂ into CH₃O by excess NO with subsequent detection of CH₃O by fluorescence assay by gas expansion (FAGE) with laser excitation at 298 nm. Detection limits of 3.8×10^8 molecules cm⁻³ were determined for CH₃O₂ for a signal-to-noise ratio of 2 and 5 min. averaging time. Noziere and Hanson (2017) reported on species RO₂ radical measurements using proton transfer ionization mass spectrometry. They utilized H₃O⁺ and water clusters H₃O⁺(H₂O)_n with n = 1–5 as adduct ions to softly ionize RO₂ radicals. The detection sensitivity of each RO₂ radical was estimated by titration with NO and varied from 0.05 to 1 cps/ppvt, with an uncertainty of a factor of 3–5.

In the present study we modified the recently developed PTR3-TOF instrument (Breitenlechner et al., 2017) utilizing NH₄⁺ clusters as adduct ions and naming this new instrument NH₄⁺-CI3-TOF. The performance of the NH₄⁺-CI3-TOF was compared to the acetate-CI-API-TOF focusing on the detection of first generation RO₂ radicals and closed-shell products including the highly oxidized products from ozonolysis of cyclohexene. Our results show a detection sensitivity for RO₂ radicals and other organic molecules (OMs) of 28 cps/ppvt utilizing the NH₄⁺-CI3-TOF which shows promise to reach carbon-closure. Thus, the results of the NH₄⁺-CI3-TOF technique significantly contribute to a more complete understanding of the reaction mechanism of gas phase ozonolysis of alkenes in the atmosphere.

2. Materials and methods

The gas-phase reaction of ozone with cyclohexene was studied in the TROPOS free-jet flow system (Berndt et al., 2015) (outer tube: length: 200 cm, 15 cm i.d. and a moveable inner tube: 9.5 mm o.d. with a 3 mm i.d. nozzle) at T = 295 ± 2 K and 1 bar pressure of purified air; see Fig. 1. The inner flow (5 L min⁻¹ STP) containing ozone diluted in purified air is injected through a nozzle into the main gas stream (95 L min⁻¹ STP) comprising the second reactant (cyclohexene) mixed in the carrier gas. Rapid mixing of the two gas streams takes place downstream the nozzle exit ensuring homogeneously mixed reactant conditions. The free-jet flow system is designed in such a way that wall losses of reaction products are negligible during the 7.9 s reaction time



Scheme 1. First steps of the ozonolysis of cyclohexene. (a) Formation of the first RO₂ radical, O₂-C₆H_{9-x}(OOH)_xO₂ with x = 0, (b) Intramolecular H-abstraction and subsequent formation of O₂-C₆H_{9-x}(OOH)_xO₂ with x = 1 and O-C₅H_{9- α} (OOH) _{α} O₂ with α = 1 according to Berndt et al. (2015).

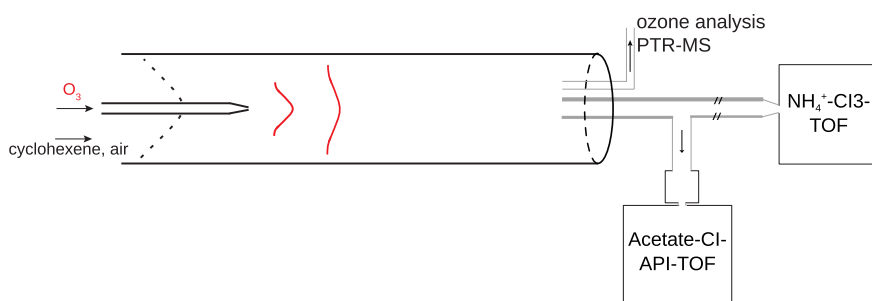


Fig. 1. Schematic of the TROPOS free-jet flow reactor including the sampling of gas phase compounds: Ozone (Thermo Environmental Instruments 49C), cyclohexene (PTR-MS; HS PTR-MS 500, Ionicon), organic product molecules (OM) NH_4^+ -CI3-TOF and highly oxidized organic molecules (HOMs) Acetate-CI-API-TOF. The red lines illustrate the development of the ozone/cyclohexene plume.

(t) given by the distance between the nozzle and the sampling point of the mass spectrometers.

Ozone was produced by passing air through an ozone generator (UVP OG-2). The reactant gas cyclohexene was prepared in a glass flask by diluting the head space of pure C_6H_{10} (Fluka $\geq 99.5\%$) with helium. Air was taken from a PSA (pressure swing adsorption) unit with further purification by activated charcoal and a 4 \AA molecular sieve. The water vapor concentration of the purified (dry) air was $< 10^{13}$ molecules cm^{-3} as checked by means of FT-IR measurements.

The ozone concentration was continuously measured at the outflow of the reactor by an ozone monitor (Thermo Environmental Instruments 49C) and was held constant at 1.0×10^{12} molecules cm^{-3} during the experiment. A proton transfer reaction - mass spectrometer (PTRMS; HS PTR-QMS 500, Ionicon) served as a real-time monitor for cyclohexene, which was varied from 0.1 to 570 ppbv.

The amount of reacted cycloalkene by ozonolysis was calculated according to $\text{reacted}[\text{cycloalkene}] = k(\text{cyclohexene} + \text{O}_3) \times [\text{O}_3] \times [\text{cyclohexene}] \times t$. Low reactant conversion smaller than 1% justified this approach. The needed rate coefficient was taken from [Greene and Atkinson \(1992\)](#), $k(\text{cyclohexene} + \text{O}_3) = 7.46 \times 10^{-17} \text{ cm}^3 \text{ molecule}^{-1} \text{ s}^{-1}$.

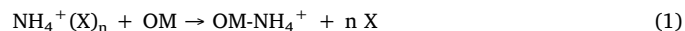
3. Product detection and determination of concentrations

The oxidation products were measured by two different chemical ionization mass spectrometer (CIMS) instruments, i.e. a NH_4^+ -CI3-TOF utilizing NH_4^+ ion chemistry and an acetate-CI-API-TOF using CH_3COO^- ion chemistry. The NH_4^+ -CI3-TOF and the acetate-CI-API-TOF sampled from the center flow of the free-jet flow system through a short sampling inlet with an inner diameter of 1.6 cm connecting the acetate-CI-API-TOF through a 90° knee and the ammonium-CI3-TOF through a straight connector coupled to a 77 cm long PTFE line (inner diameter 1 cm). Both instruments were sampling gas with a rate of 10 L min^{-1} (STP), respectively. The short acetate-CI-API-TOF inlet is very similar to that used in previous experiments ([Berndt et al., 2016](#)). Therefore, the same 12% diffusion loss for oxidized molecules was assumed as determined earlier, $f_{\text{inlet}} = 0.88$. Diffusion controlled wall loss of the CI3 inlet was calculated according to the 1st order wall loss with the rate coefficient $k_{\text{wall}} = 3.65 \times D/r^2$, $r = 0.475 \text{ cm}$ and a diffusion coefficient $D = 0.1 \text{ cm}^2 \text{ s}^{-1}$ applied for all organic radicals ([Tang et al., 2015](#)). With a bulk residence time of 0.38 s (sampling line and 77 cm PTFE line) a radical loss in the inlet of 50% follows, which was taken into account for estimating radical concentrations. Wall loss of closed-shell species was assumed to be negligible due to the inertness of the PTFE surface being the predominant surface material.

3.1. The ammonium CI3-TOF

NH_4^+ has already been used previously in proton-transfer reaction mass spectrometry (PTR-MS) as discussed by [Lindinger et al. \(1998\)](#). NH_3 has a much higher proton affinity than water, $204 \text{ kcal mol}^{-1}$ instead of $166 \text{ kcal mol}^{-1}$, it can only transfer a proton to compounds having a proton affinity in excess of $204 \text{ kcal mol}^{-1}$. Therefore NH_4^+ is

more selective than H_3O^+ in ionizing compounds present in a gas mixture, and thus NH_4^+ has been used to discriminate between compounds having suitable different proton affinities ([Lindinger et al., 1998](#)). [Blake et al. \(2006\)](#) reported that NH_4^+ and the “contaminant” $\text{NH}_4^+(\text{NH}_3)$ ions exiting a radioactive ion source produce association complexes such as $\text{NH}_4^+(\text{OM})$ with oxygenated molecules (OM) while pure hydrocarbon compounds such as benzene, toluene, butene show no ion products at all. It is well known that third body association reactions between ions and molecules are slow especially at enhanced collision energies. In contrast, exothermic ligand switching reactions are fast and proceed at every collision. Therefore we modified the recently developed PTR3-TOF ([Breitenlechner et al., 2017](#)) utilizing NH_4^+X_n clusters as adduct ions, which exchange the ligand X being mainly NH_3 (and also H_2O ; $n = 1, 2$) at every collision with an oxygenated molecule (OM) according to equation (1).



The ammonium-CI3-TOF (chemical ionization-time-of-flight) mass spectrometer is shown in [Fig. 2](#). NH_4^+X_n reagent ions were produced in the corona discharge ion source from NH_3 and H_2O introduced as chemical ionization (CI) gas. PTR3-TOF uses normally a mixture of H_2O and nitrogen as CI gas to generate prevalingly $\text{H}_3\text{O}^+(\text{H}_2\text{O})_n$ cluster ions

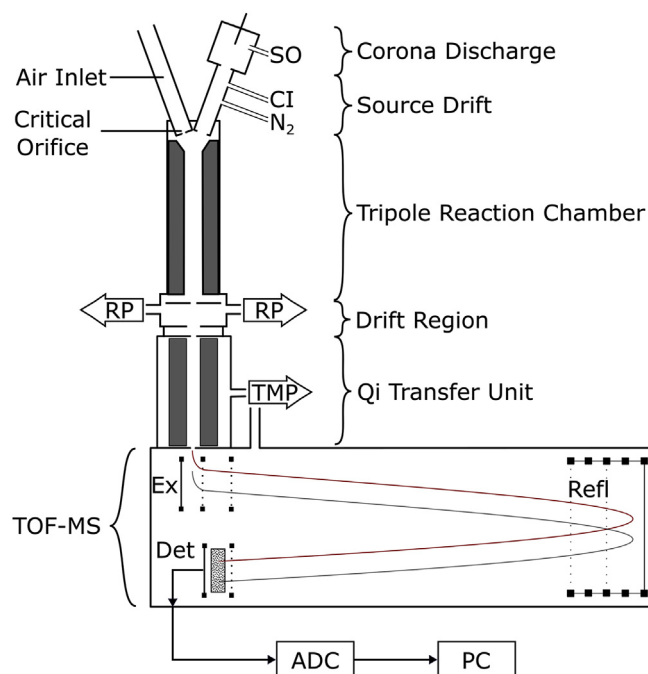


Fig. 2. Schematics of the NH_4^+ -CI3-TOF consisting of a corona discharge ion source, a source drift region, a tripole reaction chamber, a drift region, a quadrupole (Qi) transfer unit and a TOF-MS containing an extractor (Ex), a reflector (Refl), and an ion detector (Det). Roughing pumps (RP) and turbo molecular pumps (TMP) are used to manage the inlet flow through the critical orifice, the Nitrogen (N_2) and the chemical ionization (CI) gas flow.

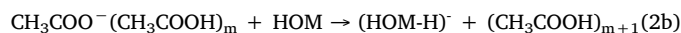
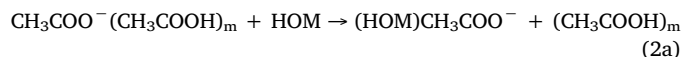
(Breitenlechner et al., 2017). Here NH_3 was added into the ion source taking 0.7 mL min^{-1} (STP) from the head space of a liquid ammonia water mixture. (Ammonium hydroxide solution 28.0–30.0% NH_3 basis, ACS reagent, Sigma-Aldrich). From the center of the 10 L min^{-1} laminar inlet gas flow approximately 2 L min^{-1} are transferred into the tripole reaction chamber through a critical orifice. Small lateral bores in close proximity to the critical orifice ensure that the sheath gas is pumped out symmetrically around the core flow entering the instrument to minimize wall contact of the sample gas. This core-sampling approach is essential to minimize wall losses of e.g. peroxy radicals (RO_2). The $\text{NH}_4^+ \text{X}_n$ cluster ion distribution can be regulated by the rf-amplitude (rf stands for radio frequency) applied to the tripole rods. The gas flow through the tripole exit lens (Fig. 2) leads to a pressure drop from 80 mbar to 2 mbar in the drift region preparing the coupling of the tripole reaction chamber to a quadrupole (Qi) interfaced LToF mass spectrometer (TOFWERK AG, Thun, Switzerland). In this region the ions motion is dominated by the electric field at 2 mbar similar as in a standard PTR-MS drift tube. The time ions spend in this region (typically $20 \mu\text{s}$) and the numbers of collisions with the sample gas molecules is small compared to the overall reaction time but if the collision energy is too high adduct ions fragment hence reducing the OM sensitivities.

We achieved highest sensitivities of $(\text{OM})\text{NH}_4^+$ adduct ions at low rf-amplitudes and low voltage settings in the drift region. In addition, the observed primary ion distribution is influenced by the quadrupole (Qi) interface of the mass spectrometer, mostly by suppressing the signal intensity of light ions due to the low-mass cutoff of rf-only ion guides. The ammonium-CI3-TOF was calibrated with a gas standard containing 1 ppm 3-hexanone in nitrogen, which was dynamically diluted by a factor of 1000 in VOC-free air to contain 1 ppb 3-hexanone. Duty cycle corrected counts per second (dcps, normalized to $m/z = 101$); are used in order to compensate for the mass-dependent transmission of the TOF mass spectrometer ($dcps(i) = cps(i) \sqrt{101/m_i}$) (Breitenlechner et al., 2017). For 3-hexanone and heptanone we obtained a sensitivity of 28 dcps/ppbv, which is in agreement with the calculated sensitivity taking into account the duty cycle corrected $\text{NH}_4^+ \text{X}_n$ adduct ion count rates, the pressure and the reaction time in the reaction chamber (80 mbar; 4 ms) and using $2\text{--}3 \times 10^{-9} \text{ cm}^3 \text{ s}^{-1}$ as a fast ligand switching reaction rate constant close to the collisional limit value (Viggiano et al., 1989). Consequently, only lower end product concentrations can be given using a sensitivity of 28 dcps/ppbv. We used a liquid calibration unit (LCU) from Ionicon analytik to calibrate adipaldehyde and glutaraldehyde, which are oxidation products from cyclohexene ozonolysis (Aschmann et al., 2003). Aqueous standards were prepared by diluting $2 \mu\text{l}$ of adipaldehyde (95%, Activate Scientific) and glutaraldehyde (70%, Sigma-Aldrich) in 250 mL purified water. $5 \mu\text{L min}^{-1}$ of the aqueous standard mixture was evaporated into a gas stream of purified synthetic air (4 slpm) resulting in calibration gas standards containing 2 ppbv adipaldehyde or glutaraldehyde, respectively. The sensitivities of adipaldehyde and glutaraldehyde were found to be 0.53 and 0.56 relative to 3-hexanone. Adding purified water into the LCU allowed to change the relative humidity, which resulted in a slight water dependence of the sensitivity of less than 10%. For estimating adipaldehyde and glutaraldehyde concentrations we used the calibration results. For HOMs no standards are available and we assumed a fast reaction rate constant therefore using the sensitivity of 3-hexanone. The diffusion controlled wall losses for the CI3-TOF inlet were calculated to be 50%, which was taken into account for estimating the radical concentrations. Overall an uncertainty of the product concentrations is assumed to be less than a factor of two.

3.2. The ACETATE-CI-API-TOF

The acetate-CI-API-TOF (chemical ionization-atmospheric pressure interface-time-of-flight) mass spectrometer (Airmodus, ToFwerk)

sampled from the center flow with a rate of 10 L min^{-1} (STP). A flow of 2 mL min^{-1} of air over an acetic acid sample was added to 35 L min^{-1} (STP) flow of purified air producing the CH_3COOH containing sheath air that produces the reagent ions $(\text{CH}_3\text{COOH})_m \text{CH}_3\text{COO}^-$ ($m = 0, 1, 2$) after ionization with a ^{241}Am foil. The ions from the sheath flow are electrostatically forced into the sample flow (in the middle of the CI-inlet) without mixing of both streams. Especially highly oxidized multifunctional organic compounds (HOMs) are able to form stable $(\text{HOM})\text{CH}_3\text{COO}^-$ adduct ions as well as deprotonation products $(\text{HOM-H})^-$ according to equations (2a) and (2b), respectively.



Concentrations of HOMs and other detectable products (radicals and closed-shell products) were determined according to equation (3). The values given in the brackets are duty cycle corrected measured ion signals.

$$[\text{HOM}] = f_{\text{HOM}} \frac{[(\text{HOM} - \text{H})^-] + [(\text{HOM})\text{CH}_3\text{COO}^-]}{[\text{CH}_3\text{COO}^-(\text{CH}_3\text{COO})_m]} \quad (3)$$

Calibration of HOMs is not possible due to lack of reference standards. The calibration factor f_{HOM} was calculated $f_{\text{HOM,calc}} = 1/(k \times t \times f_{\text{inlet}}) = (1.3\text{--}2.8) \times 10^9 \text{ molecules cm}^{-3}$, where k is the rate coefficient of the ion-molecule reaction, $k = (2\text{--}3) \times 10^{-9} \text{ cm}^3 \text{ molecule}^{-1} \text{ s}^{-1}$, assuming fast ion-molecule rate coefficients close to the collision limit (Viggiano et al., 1997; Mackay and Bohme, 1978), t is the corresponding reaction time $t = 0.2\text{--}0.3 \text{ s}$, $f_{\text{inlet}} = 0.88$ stands for the diffusion loss of 12% in the sample tube, see Berndt et al., 2016. By practical reasons, the value f_{HOM} was set equal to $f_{\text{H}_2\text{SO}_4, \text{exp}} = 1.85 \times 10^9 \text{ molecules cm}^{-3}$ obtained from the absolute H_2SO_4 calibration using $(\text{HNO}_3)_n \text{NO}_3^-$, $n = 0, 1, 2$ as the reagent ions (Berndt et al., 2014). The value $f_{\text{HOM}} = f_{\text{H}_2\text{SO}_4, \text{exp}} = 1.85 \times 10^9 \text{ molecules cm}^{-3}$ is well in line with the range of $f_{\text{HOM,calc}} = (1.3\text{--}2.8) \times 10^9 \text{ molecules cm}^{-3}$ that represents the lower limit of the calibration factor. Consequently, only lower end product concentrations can be stated based on equation (3) applying $f_{\text{HOM}} = f_{\text{H}_2\text{SO}_4, \text{exp}}$. The total uncertainty of the lower end product concentrations is assumed to be not higher than a factor of two considering the uncertainty of f_{HOM} and possible inaccuracy connected with the duty cycle correction.

4. Results and discussion

Fig. 3 shows the mass spectrum obtained with the NH_4^+ -CI3-TOF from the ozonolysis of cyclohexene ($[\text{O}_3] = 2.25 \times 10^{12} \text{ molecules cm}^{-3}$, $[\text{cyclohexene}] = 2.0 \times 10^{12} \text{ molecules cm}^{-3}$) with and without the addition of $1.23 \times 10^{16} \text{ molecules cm}^{-3}$ propane as OH-radical scavenger.

The most intense product peaks from the pure O_3 reaction (when propane was added) are 104.107 m/z ($\text{C}_5\text{H}_{10}\text{O})\text{NH}_4^+$, 118.086 m/z ($\text{C}_5\text{H}_8\text{O}_2)\text{NH}_4^+$, 132.102 m/z ($\text{C}_6\text{H}_{10}\text{O}_2)\text{NH}_4^+$, 148.097 m/z ($\text{C}_6\text{H}_{10}\text{O}_3)\text{NH}_4^+$ and 150.075 m/z ($\text{C}_5\text{H}_8\text{O}_4)\text{NH}_4^+$. This is in very good agreement with Aschmann et al. (2003), who identified the main ozonolysis products as pentanal ($\text{C}_5\text{H}_{10}\text{O}$), glutaraldehyde ($\text{C}_5\text{H}_8\text{O}_2$), adipaldehyde ($\text{C}_6\text{H}_{10}\text{O}_2$), peracid ($\text{C}_5\text{H}_8\text{O}_4$), and attributed the signal at ($\text{C}_6\text{H}_{10}\text{O}_3$) to the secondary ozonide (SOZ) and/or hydroxy dicarbonyl compounds. Subtracting the product ion signals in the presence of propane from the one without the addition of propane we obtained the individual product ion signals for the OH + cyclohexene reaction only. The product ion signals from OH radical reactions are 132.102 m/z ($\text{C}_6\text{H}_{10}\text{O}_2)\text{NH}_4^+$, 134.118 m/z ($\text{C}_6\text{H}_{12}\text{O}_2)\text{NH}_4^+$, 149.105 ($\text{C}_6\text{H}_{11}\text{O}_3)\text{NH}_4^+$, 150.113 ($\text{C}_6\text{H}_{12}\text{O}_3)\text{NH}_4^+$ (see Table 1).

We attribute the observed $(\text{C}_6\text{H}_{11}\text{O}_3)\text{NH}_4^+$ ion signal solely to the first peroxy radical arising from the OH radical addition to cyclohexene and subsequent O_2 addition, i.e. $\text{HO-C}_6\text{H}_{10}\text{O}_2$ (Aschmann et al., 2012).

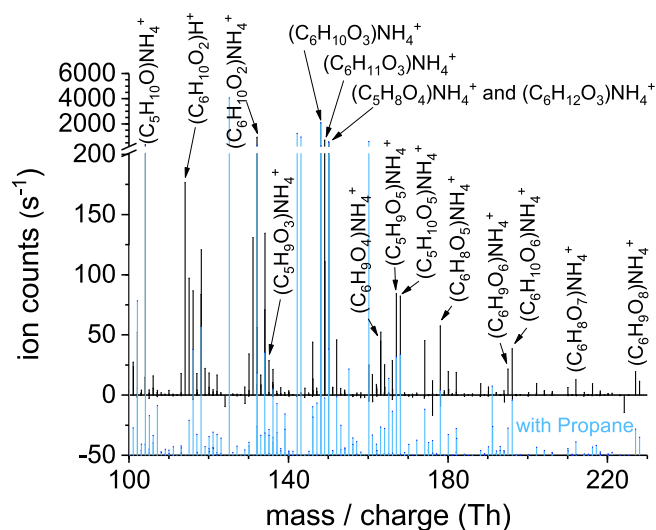


Fig. 3. NH_4^+ -CI3-TOF Mass spectra from the ozonolysis of cyclohexene in the mass/charge range of observed products (100–230 Th) in the absence (upper part) or presence (lower part in blue) of propane as OH-radical scavenger. $[\text{O}_3] = 2.25 \times 10^{12}$, $[\text{C}_6\text{H}_{10}] = 2.0 \times 10^{12}$ and $[\text{C}_3\text{H}_8] = 1.23 \times 10^{16}$ molecules cm^{-3} and a reaction time of 7.9 s.

Table 1 shows observed product ion signals converted to concentrations and relative amounts, the proposed composition and the contribution either from ozone or OH chemistry.

The first ten different m/z product peaks converted to concentrations sum up to 93% of the observed cyclohexene products resulting from the first steps of the cyclohexene ozonolysis including the simultaneous OH radical reaction. The remaining 7% are distributed over m/z peaks that can be attributed to highly oxidized organic molecules (HOMs) predominately highly oxidized peroxy radicals (RO_2) and some

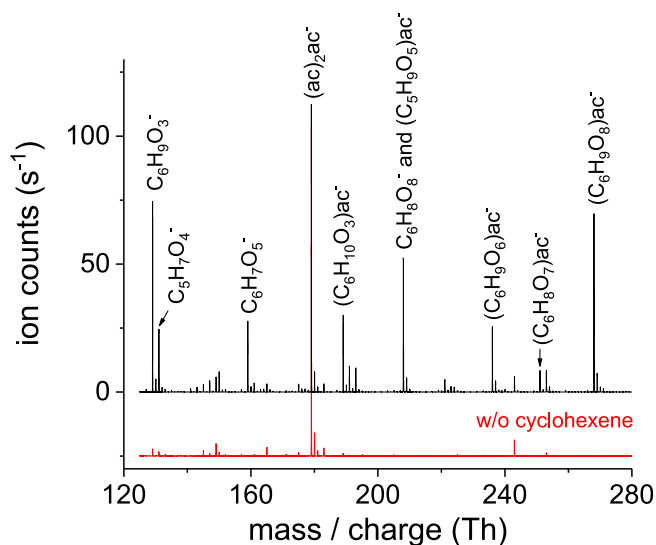


Fig. 4. Acetate-CI-API-TOF mass spectra from the ozonolysis of cyclohexene in the mass/charge range of observed products (120–280 Th). In the absence (upper part) or presence (lower part) of cyclohexene. $[\text{O}_3] = 2.25 \times 10^{12}$, $[\text{C}_6\text{H}_{10}] = 2.0 \times 10^{12}$, reaction time of 7.9 s.

closed shell products. The first RO_2 radical ($x = 0$) is formed after ring cleavage of the primary ozonide followed by O_2 addition and OH radical release, see Scheme 1. This RO_2 radical undergoes in the absence of bimolecular reactions internal H-abstraction and subsequent formation of either $\text{O}_2\text{-C}_6\text{H}_9\text{-x}(\text{OOH})_x\text{O}_2$ via direct O_2 addition or $\text{O-C}_5\text{H}_9\text{-}\alpha(\text{OOH})_2\text{O}_2$ via decomposition (CO splitting-off) and subsequent O_2 addition (Berndt et al., 2015). In Fig. 3 and Table 1 the m/z peaks of NH_4^+ adduct ions of peroxy radicals ($x = 0$ –2) and ($\alpha = 1$) are shown together with closed shell HOMs such as $(\text{C}_5\text{H}_8\text{O}_4)\text{NH}_4^+$, $(\text{C}_5\text{H}_{10}\text{O}_5)\text{NH}_4^+$, $(\text{C}_6\text{H}_{10}\text{O}_6)\text{NH}_4^+$, $(\text{C}_6\text{H}_8\text{O}_7)\text{NH}_4^+$. The amount of reacted

Table 1

List of products observed with the NH_4^+ -CI3-TOF.

observed m/z (Th)	adduct ion	proposed compound	ref	Ion-intensities (cps)		f	Concentrations ^a (molecules cm^{-3})		rel. (%)
				From O_3	OH		From O_3	OH	
104.107	$(\text{C}_5\text{H}_{10}\text{O})\text{NH}_4^+$	pentanal	b	362		1	3.2×10^8		5.6%
116.107	$(\text{C}_6\text{H}_{10}\text{O})\text{NH}_4^+$			87		1	7.2×10^7		1.3%
118.086	$(\text{C}_5\text{H}_8\text{O}_2)\text{NH}_4^+$	glutaraldehyd	b	84		1.8	1.2×10^8		2.2%
132.102	$(\text{C}_6\text{H}_{10}\text{O}_2)\text{NH}_4^+$	adipaldehyde	b	343	602	1.9	5.0×10^8	8.8×10^8	24.8%
134.081	$(\text{C}_5\text{H}_8\text{O}_3)\text{NH}_4^+$	oxo-acid	b	71		1	5.5×10^7		1.0%
134.118	$(\text{C}_6\text{H}_{12}\text{O}_2)\text{NH}_4^+$	hydroxycarbonyl	b	18	116	1	1.4×10^7	8.9×10^7	1.8%
148.097	$(\text{C}_6\text{H}_{10}\text{O}_3)\text{NH}_4^+$	SOZ / hydroxy dicarbonyls	b	2064		1	1.5×10^9		26.9%
149.105	$(\text{C}_6\text{H}_{11}\text{O}_3)\text{NH}_4^+$	HO- $\text{C}_6\text{H}_{10}\text{-O}_2$ radical	b		662	2		9.7×10^8	17.2%
150.075	$(\text{C}_5\text{H}_8\text{O}_4)\text{NH}_4^+$	peracid / hydroxy carbonyl	b,c	558		1	4.1×10^8		7.2%
150.113	$(\text{C}_6\text{H}_{12}\text{O}_3)\text{NH}_4^+$			88	336	1	6.4×10^7	2.4×10^8	5.5%
									93.4%
163.084	$(\text{C}_6\text{H}_9\text{O}_4)\text{NH}_4^+$	$x=0$ radical	–	23	21	2	3.2×10^7	2.9×10^7	1.09%
164.092	$(\text{C}_6\text{H}_{10}\text{O}_4)\text{NH}_4^+$	hydroperoxid of $x=0$	–	22		1	1.5×10^7		0.27%
167.079	$(\text{C}_5\text{H}_9\text{O}_5)\text{NH}_4^+$	$x=1$ radical	c	84		2	1.2×10^8		2.06%
168.087	$(\text{C}_5\text{H}_{10}\text{O}_5)\text{NH}_4^+$	hydroperoxid of $x=1$		82		1	5.6×10^7		1.00%
178.071	$(\text{C}_6\text{H}_8\text{O}_5)\text{NH}_4^+$	hydroxycarbonyl	c	57		1	3.8×10^7		0.68%
195.074	$(\text{C}_6\text{H}_9\text{O}_6)\text{NH}_4^+$	$x=1$ radical	c	22		2	2.8×10^7		0.50%
196.082	$(\text{C}_6\text{H}_{10}\text{O}_6)\text{NH}_4^+$	hydroperoxid of $x=1$		39		1	2.5×10^7		0.44%
227.064	$(\text{C}_6\text{H}_9\text{O}_8)\text{NH}_4^+$	$x=2$ radical	c	19		2	2.2×10^7		0.40%
228.071	$(\text{C}_6\text{H}_{10}\text{O}_8)\text{NH}_4^+$	hydroperoxid of $x=2$		12		1	7.1×10^6		0.13%
									6.6%
				measured:			3.4×10^9	2.2×10^9	5.6×10^9
				calculated:			2.7×10^9	1.8×10^9	4.5×10^9

^a Concentrations are determined from observed ion intensities (cps), corrected for duty cycle and wall losses ($f = 1$ for closed shell species and $f = 2$ for radicals) and multiplied with the calibration factor $c = 2.48 \times 10^7/28 = 8.85 \times 10^5$ molecules cm^{-3} dcps $^{-1}$. Calibration of glutaraldehyde and adipaldehyde inferred correction factors $f = 1.8$ and 1.9 respectively.

^b Aschmann et al. (2003).

^c Berndt et al. (2015).

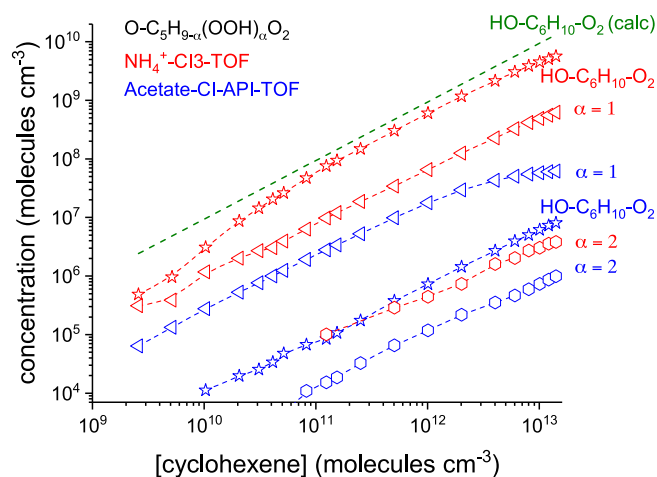


Fig. 5. RO₂ radical (O-C₅H_{9-α}(OOH)_αO₂ for α = 1, 2) and OH-C₆H₁₀-O₂ concentrations measured with the NH₄⁺-CI3-TOF (in red) and the acetate-CI-API-TOF (in blue) as a function of cyclohexene. Concentrations obtained by acetate-CI-API-TOF represent lower end values. Calculated OH-C₆H₁₀-O₂ concentrations for the reaction time of 7.9 s are given as green dashed line. [O₃] = 2.3 × 10¹² molecules cm⁻³.

cyclohexene was calculated to be 4.45 × 10⁹ molecules cm⁻³ (2.65 × 10⁹ from ozonolysis and 1.8 × 10⁹ molecules cm⁻³ from the OH radical reaction). This value is in excellent agreement with the concentrations of all observed ozonolysis products as given in Table 1 summing up to 5.6 × 10⁹ molecules cm⁻³.

Fig. 4 shows the corresponding mass spectra obtained with the acetate-CI-API-TOF from the ozonolysis of cyclohexene in the mass/charge range of 120–280 Th, in the absence (upper part) or presence (lower part) of cyclohexene. The acetate-CI-API-TOF has high sensitivity for HOMs but loses dramatically sensitivity for low oxygen containing molecules such as the first step products.

Fig. 5 compares RO₂ radical concentrations (O-C₅H_{9-α}(OOH)_αO₂ formed after CO splitting-off for α = 1, 2) and OH-C₆H₁₀-O₂ radical concentrations measured with the NH₄⁺-CI3-TOF and the acetate-CI-API-TOF as a function of cyclohexene. The RO₂ concentrations increase proportionally with increasing cyclohexene as expected in this concentration range (Berndt et al., 2015).

The observed HO-C₆H₁₀-O₂ radical concentration observed by the ammonium-CI-TOF is in excellent agreement with the calculated radical concentrations (within a factor of two). The acetate-CI-API-TOF shows qualitatively the same behavior of the RO₂ radical concentrations as a function of cyclohexene concentration. The absolute values of HO-C₆H₁₀-O₂, however, are 2–3 orders of magnitude smaller indicating a distinct lower sensitivity of the acetate-CI-API-TOF for this RO₂ radical with a rather low oxygen atom number (RO₂ radicals with no OOH group). For the more oxidized RO₂ radicals O-C₅H_{9-α}(OOH)_αO₂ with α = 1, 2 from the ozone reactions the agreement between both CIMS instruments, one using positive and the other one negative ion chemistry, is remarkably good. The NH₄⁺ ionization yielded about three times higher concentrations compared with the results from the CH₃COO⁻ ionization for the RO₂ radical with α = 1 (RO₂ radicals with a single OOH group) and a factor less than two for that with α = 2 (RO₂ radicals with two OOH groups). Almost the same result was obtained for the RO₂ radical concentrations of O,O-C₆H_{9-x}(OOH)_xO₂ with x = 0, 1, 2, 3 formed via direct O₂ addition, see Fig. 6.

While the CH₃COO⁻ ionization does not show a signal for x = 0 (RO₂ radicals with no OOH group), the agreement becomes far better, differing only by a factor of three for x = 1 (RO₂ radicals with a single OOH group) and reaching almost a one to one agreement for x = 2 (RO₂ radicals with two OOH groups). For the rather low concentrations of the x = 3 radical (less than 1 × 10⁶ molecules cm⁻³), the NH₄⁺-CI3-TOF could not detect a reliable signal above the noise level at that mass.

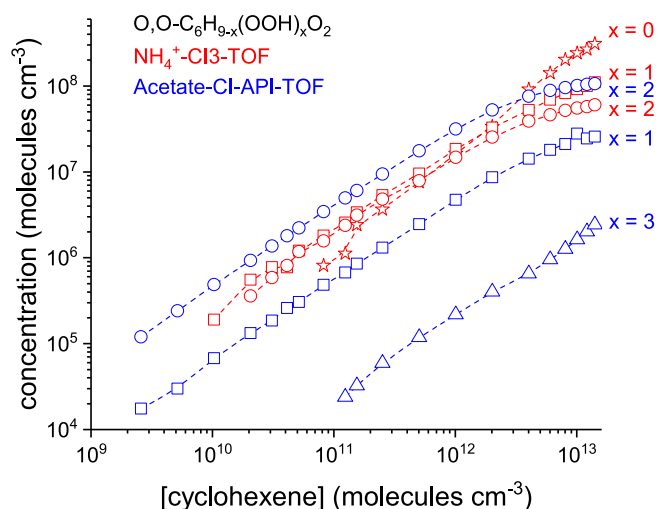


Fig. 6. RO₂ radical (O,O-C₆H_{9-x}(OOH)_xO₂ formed via direct O₂ addition for x = 0, 1, 2, 3) concentrations from cyclohexene ozonolysis measured with the NH₄⁺-CI3-TOF (in red) and the acetate-CI-API-TOF (in blue) as a function of cyclohexene. Concentrations obtained by acetate-CI-API-TOF represent lower end values. [O₃] = 2.3 × 10¹² molecules cm⁻³. Reaction time: 7.9 s.

It can be concluded that the acetate technique and the ammonium CI3-TOF are in remarkable good agreement for RO₂ radicals with at least one OOH group. For RO₂ radicals not containing any OOH group the acetate technique can considerably underestimate RO₂ concentrations.

Fig. 7 compares C₆ closed shell product concentrations measured with both CIMS instruments as a function of cyclohexene. Also here, the closed shell product concentrations increase as a function of cyclohexene concentration as expected from former experiments (Berndt et al., 2015). Again the acetate technique underestimates the closed shell compounds containing 3 oxygens (C₆H₁₀O₃) by two orders of magnitude compared to the ammonium-CI3. C₆H₁₀O₃ products were tentatively identified as SOZ and/or hydroxy carbonyls (Aschmann et al., 2003). The agreement becomes far better for highly oxidized closed shell products reaching almost a one to one line for C₆H₈O₇. For the C₆H₈O₉ the ammonium CI3-TOF was not sensitive enough.

Fig. 8 compares so-called dimer concentrations from cyclohexene ozonolysis comprising 11 or 12 carbon atoms. They originate most likely from the observed RO₂ radicals as discussed by Berndt et al.

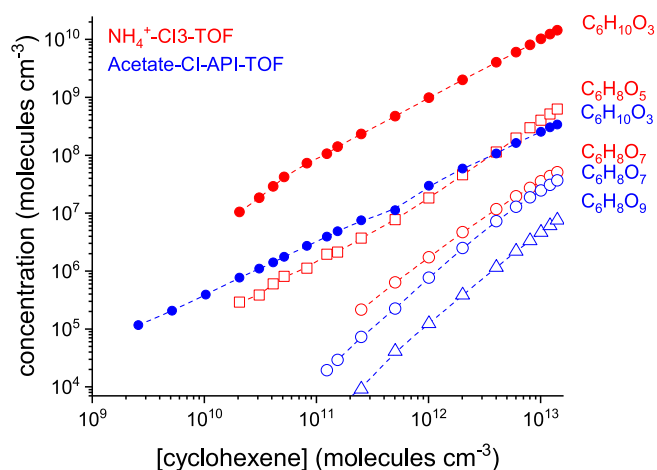


Fig. 7. C₆ closed shell product concentrations from cyclohexene ozonolysis measured with NH₄⁺-CI3-TOF (in red) and the acetate-CI-API-TOF (in blue) as a function of cyclohexene. Concentrations obtained by acetate-CI-API-TOF represent lower end values. [O₃] = 2.3 × 10¹² molecules cm⁻³, reaction time: 7.9 s.

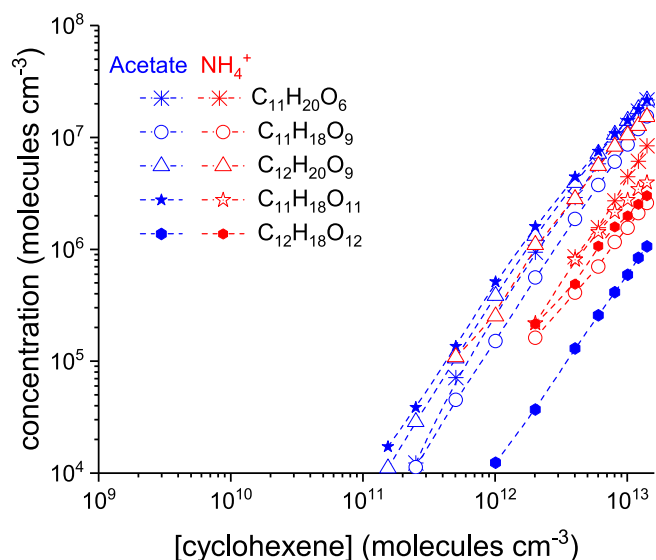


Fig. 8. C_{11} - and C_{12} -dimer concentrations from cyclohexene ozonolysis measured with the ammonium-CI3-TOF (in red) and with the acetate-CI-API-TOF (in blue) as a function of cyclohexene. Concentrations obtained by acetate-CI-API-TOF represent lower end values. $[O_3] = 2.3 \times 10^{12}$ molecules cm^{-3} , reaction time: 7.9 s.

(2015). Their formation pathways are still under investigations. The concentrations of $C_{11}H_{20}O_6$, $C_{11}H_{18}O_9$, $C_{12}H_{20}O_9$, $C_{11}H_{18}O_{11}$, $C_{12}H_{18}O_{12}$ increase as a function of cyclohexene and both instruments agree within a factor of 2–3 for the respective dimers.

5. Conclusions

We have demonstrated that the NH_4^+ -CI3-TOF utilizing NH_4^+ adduct ion chemistry detects with high sensitivity most if not all products of cyclohexene ozonolysis: peroxy radicals (RO_2), highly oxidized organic molecules (HOMs) and other oxidized product molecules (OMs) such as aldehydes, hydroxyl-carbonyls, peroxy-carboxylics and hydroperoxides. Product ion signals were simultaneously observed by the NH_4^+ -CI3-TOF and the acetate-CI-API-TOF. Both instruments agree within a factor of two for HOMs. For OMs not containing an OOH group the acetate technique can considerably underestimate OM concentrations by 2–3 orders of magnitude. The NH_4^+ -CI3-TOF is able to measure all peroxy radicals (RO_2) simultaneously reaching limit of detections of typically 2×10^5 molecules cm^{-3} (e.g. $OH-C_6H_{10}-O_2$ radical, background signal 5 cps, $S/N = 2$, integration time 10 min.) With such a low limit of detection the application of this technique is not limited to laboratory studies of organic radicals. The versatility and sensitivity of the NH_4^+ -CI3-TOF technique is high enough to apply this technique not only for laboratory based studies, or more generally for oxidation reactions, but also for environmental measurements in real-time.

Author contributions

The manuscript was written through contributions of all authors. All authors have given approval to the final version of the manuscript.

Funding sources

Austrian Research Funding Association (FFG. Project Number 846050).

Acknowledgment

We thank K. Pielok for technical assistance and the Austrian

Research Funding Association (FFG. Project Number 846050) for financial support and IONICON Analytik GmbH for in-kind contributions within the funded project.

Appendix A. Supplementary data

Supplementary data related to this article can be found at <http://dx.doi.org/10.1016/j.atmosenv.2018.04.023>.

References

- Aschmann, S.M., Tuazon, E.C., Arey, J., Atkinson, R., 2003. Products of the gas-phase reaction of O_3 with cyclohexene. *J. Phys. Chem.* 107, 2247–2255.
- Aschmann, S.M., Arey, J., Atkinson, R., 2012. Kinetics and products of the reactions of OH radicals with cyclohexene, 1-Methyl-1-cyclohexene, cis-cyclooctene, and cis-cyclo-decene. *J. Phys. Chem.* 116, 95077–99515.
- Berndt, T., Jokinen, T., Sipilä, M., Mauldin III, R.L., Herrmann, H., Stratmann, F., Junninen, H., Kulmala, M., 2014. H2SO4 formation from the gas-phase reaction of stabilized Criegee Intermediates with SO_2 : influence of water vapour content and temperature. *Atmos. Environ.* 89, 603–612.
- Berndt, T., Richters, S., Kaethner, R., Voigtländer, J., Stratmann, F., Sipilä, M., Kulmala, M., Herrmann, H., 2015. Gas-phase ozonolysis of cycloalkenes: formation of highly oxidized RO_2 radicals and their reactions with NO , NO_2 , SO_2 , and other RO_2 radicals. *J. Phys. Chem.* 119, 10336–10348.
- Berndt, T., Richters, S., Jokinen, T., Hyttinen, N., Kurten, T., Otkjaer, R.V., Kjaergaard, H.G., Stratmann, F., Herrmann, H., Sipilä, M., Kulmala, M., Ehn, M., 2016. Hydroxyl radical-induced formation of highly oxidized organic compounds. *Nat. Commun.* 7, 13677.
- Blake, R.S., Wyche, K.P., Ellis, A.M., Monks, P.S., 2006. Chemical ionization reaction time-of-flight mass spectrometry: multi-reagent analysis for determination of trace gas composition. *Int. J. Mass Spectrom.* 254, 85–93.
- Breitenlechner, M., Fischer, L., Hainer, M., Heinritzi, M., Curtius, J., Hansel, A., 2017. PTR3: an instrument for studying the lifecycle of reactive organic carbon in the atmosphere. *Anal. Chem.* 89 (11), 5824–5831.
- Crouse, J.D., Nielsen, L.B., Jørgensen, S., Kjaergaard, H.G., Wennberg, P.O., 2013. Autoxidation of organic compounds in the atmosphere. *J. Phys. Chem. Lett.* 4, 3513–3520.
- Donahue, N.M., Kroll, J.H., Pandis, S.N., Robinson, A.L., 2012. A two-dimensional volatility basis set – Part 2: diagnostics of organic-aerosol evolution. *Atmos. Chem. Phys.* 12, 615–634.
- Ehn, M., Kleist, E., Junninen, H., Petäjä, T., Lönn, G., Schobesberger, S., Dal Maso, M., Trimborn, A., Kulmala, M., Worsnop, D.R., Wahner, A., Wildt, J., Mentel, Th F., 2012. Gas phase formation of extremely oxidized pinene reaction products in a chamber and ambient air. *Atmos. Chem. Phys.* 12, 5113–5127.
- Ehn, M., Thornton, J.A., Kleist, E., Sipilä, M., Junninen, H., Pullinen, I., Springer, M., Rubach, F., Tillmann, R., Lee, B., Lopez-Hilfiker, F., Andres, S., Acir, I.-H., Rissanen, M., Jokinen, T., Schobesberger, S., Kangasluoma, J., Kontkanen, J., Nieminen, T., Kurtén, T., Nielsen, L.B., Jørgensen, S., Kjaergaard, H.G., Canagaratna, M., Dal Maso, M., Berndt, T., Petäjä, T., Wahner, A., Kerminen, V.-M., Kulmala, M., Worsnop, D.R., Wildt, J., Mentel, T., 2014. A large source of low-volatility secondary organic aerosol. *Nature* 506, 476–479.
- Greene, C.R., Atkinson, R., 1992. Rate constants for the gas-phase reactions of O_3 with a series of alkenes at 296 ± 2 K. *Int. J. Chem. Kinet.* 24, 803–811.
- Guenther, A.B., Jiang, H., Heald, C.L., Sakulyanontvittaya, T., Duhl, T., Emmons, L.K., Wang, X., 2012. The model of emissions of gases and aerosols from nature version 2.1 (MEGAN2.1): an extended and updated framework for modeling biogenic emissions. *Geosci. Model Dev. (GMD)* 5, 1471–1492.
- Jokinen, T., Sipilä, M., Richters, S., Kerminen, V.-M., Paasonen, P., Stratmann, F., Worsnop, D.R., Kulmala, M., Ehn, M., Herrmann, H., Berndt, T., 2014. Rapid autoxidation forms highly oxidized RO_2 radicals in the atmosphere. *Angew. Chem. Int. Ed.* 53, 14596–14600.
- Lindinger, W., Hansel, A., Jordan, A., 1998. On-line monitoring of volatile organic compounds at pptv levels by means of Proton-Transfer-Reaction Mass Spectrometry (PTR-MS) Medical applications, food control and environmental research. *Int. J. Mass Spectrom. Ion Process.* 173, 191–241.
- Mackay, G.I., Bohme, D.K., 1978. Proton-transfer reactions in nitromethane at 297 K. *Int. J. Mass Spectrom. Ion Phys.* 26, 327–343.
- Mentel, T.F., Springer, M., Ehn, M., Kleist, E., Pullinen, I., Kurtén, T., Rissanen, M.P., Wahner, A., Wildt, J., 2015. formation of highly oxidized multifunctional compounds: autoxidation of peroxy radicals formed in the ozonolysis of alkenes – deduced from Structure–Product relationships. *Atmos. Chem. Phys.* 15, 6745–6765.
- Nozière, B., Hanson, D.R., 2017. Speciated monitoring of gas-phase organic peroxy radicals by chemical ionization mass spectrometry: cross-reactions between CH_3O_2 , $CH_3(CO)O_2$, $(CH_3)_2CO_2$ and $c-C_6H_{11}O_2$. *J. Phys. Chem.* 121, 8453–8464.
- Onel, L., Brennan, A., Seakins, P.W., Whalley, L., Heard, D.E., 2017. A new method for atmospheric detection of the CH_3O_2 radical. *Atmos. Meas. Tech.* 10, 3985–4000.
- Riipinen, I., Yli-Juuti, T., Pierce, J.R., Petäjä, T., Worsnop, D.R., Kulmala, M., Donahue, N.M., 2012. The contribution of organics to atmospheric nanoparticle Growth. *Nat. Geosci.* 5, 453–458.
- Rissanen, M.P., Kurten, T., Sipilä, M., Thornton, J.A., Kangasluoma, J., Sarnela, N., Junninen, H., Jørgensen, S., Schallhart, S., Kajos, M.K., Taipale, R., Springer, M., Mentel, Th F., Ruuskanen, T., Petäjä, T., Worsnop, D.R., Kjaergaard, H.G., Ehn, M.,

2014. the formation of highly oxidized multifunctional products in the ozonolysis of cyclohexene. *J. Am. Chem. Soc.* 136, 15596–15606.
- Tang, M.J., Shiraiwa, M., Pöschl, U., Cox, R.A., Kalberer, M., 2015. Compilation and evaluation of gas phase diffusion coefficients of reactive trace gases in the atmosphere: volume 2. Diffusivities of organic compounds, pressure-normalised mean free paths, and average Knudsen numbers for gas uptake calculations. *Atmos. Chem. Phys.* 15, 5585–5598.
- Viggiano, A.A., Dale, F., Paulson, J.F., 1989. Proton transfer reactions of $H^+(H_2O)_{n=2-11}$ with methanol, ammonia, pyridine, acetonitrile, and acetone. *J. Chem. Phys.* 88, 2469–2477.
- Viggiano, A.A., Seeley, J.V., Mundis, P.L., Williamson, J.S., Morris, R.A., 1997. Rate constants for the reactions of $XO_3^-(H_2O)_n$ ($X = C, HC, \text{ and } N$) and $NO_3^-(HNO_3)_n$ with H_2SO_4 : implications for atmospheric detection of H_2SO_4 . *J. Phys. Chem.* 101, 8275–8278.